

# Proton-Observed Carbon-Edited NMR Spectroscopy in Strongly Coupled Second-Order Spin Systems

Pierre-Gilles Henry,<sup>1\*</sup> Malgorzata Marjanska,<sup>1</sup> Jamie D. Walls,<sup>2</sup> Julien Valette,<sup>3</sup> Rolf Gruetter,<sup>1</sup> and Kâmil Uğurbil<sup>1</sup>

**Proton-observed carbon-edited (POCE) NMR spectroscopy is commonly used to measure <sup>13</sup>C labeling with higher sensitivity compared to direct <sup>13</sup>C NMR spectroscopy, at the expense of spectral resolution. For weakly coupled first-order spin systems, the multiplet signal at a specific proton chemical shift in POCE spectra directly reflects <sup>13</sup>C enrichment of the carbon attached to this proton. The present study demonstrates that this is not necessarily the case for strongly coupled second-order spin systems. In such cases NMR signals can be detected in the POCE spectra even at chemical shifts corresponding to protons bound to <sup>12</sup>C. This effect is demonstrated theoretically with density matrix calculations and simulations, and experimentally with measured POCE spectra of [3-<sup>13</sup>C]glutamate. Magn Reson Med 55:250–257, 2006. © 2006 Wiley-Liss, Inc.**

**Key words:** POCE NMR spectroscopy; glutamate; strong coupling; <sup>13</sup>C editing; density matrix simulation

Carbon-13 NMR spectroscopy combined with infusion of <sup>13</sup>C-labeled substrates is a powerful tool for investigations of intermediary metabolism in living organisms. The measurement of <sup>13</sup>C label incorporation from glucose into glutamate and glutamine in the brain has provided new insights into brain energy metabolism and neurotransmitter compartmentation between neurons and glia (see Ref. 1 for a recent review).

It is generally considered that indirect detection (i.e., selective detection of signals from protons bound to <sup>13</sup>C) provides better sensitivity than direct <sup>13</sup>C detection, at least for well resolved CH<sub>2</sub> and CH<sub>3</sub> resonances (2). Although studies using direct detection have provided unique information, such as the resolved detection of C4, C3, and C2 carbon positions in glutamate and glutamine, and the detection of

different isotopomers with distinct <sup>13</sup>C-<sup>13</sup>C coupling patterns (3–5), these studies generally required relatively large volumes. In contrast, studies using indirect detection have proved very useful for investigating small areas of the brain during functional activation (6,7) or distinct brain tissue types such as gray and white matter (8,9). This advantage of increased sensitivity is coupled with the disadvantage of low spectral dispersion, which prevents resolution of the proton signals for C4-labeled glutamate and glutamine in human studies at 4 T, for example, or C3-labeled glutamate and glutamine in animal studies at 9.4 T.

Most indirect detection studies performed *in vivo* used either a proton-observed carbon-edited (POCE) sequence (as defined in Fig. 1) (10) or other sequences proposed later on (11–14). A common feature of these sequences is the ability to select specifically the signals from protons bound to <sup>13</sup>C using difference spectroscopy (editing). Signals from protons bound to <sup>13</sup>C are inverted every other scan and add coherently in the difference spectrum, whereas signals from protons that are not attached to <sup>13</sup>C are unaffected by the <sup>13</sup>C inversion pulse and are subtracted out in the difference spectrum. Most importantly, the proton signal intensity (integral) at a given chemical shift is commonly assumed to directly reflect the <sup>13</sup>C isotopic enrichment of the carbon attached to this proton. This property is critical for metabolic studies in which incorporation of <sup>13</sup>C label is quantitated separately for different carbon positions.

The performance of POCE is readily described for first-order weakly coupled systems ( $\Delta\delta_H \gg J_{HH}$ ) using the classic vector model (15) or product operator formalism (10,14). To the best of our knowledge, however, second-order strong coupling effects on the performance of POCE have not been reported to date. Strongly coupled systems are common at magnetic fields used for *in vivo* studies due to the small chemical shift dispersion achieved. For example, the H4 and H3 protons of glutamate cannot be considered to be weakly coupled, even at 9.4 T. Since the evolution of transverse magnetization during a pulse sequence results in partial coherence transfer within strongly coupled systems (but not for weakly coupled protons), the editing selectivity of POCE may be affected in strongly coupled systems.

The aim of the present study was to evaluate the editing performance of POCE when applied to strongly coupled <sup>1</sup>H spin systems. Strong coupling effects in POCE spectra were investigated theoretically for a simple hypothetical CH-CH spin system. These effects were then studied in [3-<sup>13</sup>C]glutamate using simulated and measured POCE spectra at different field strengths. Implications for the quantification of POCE spectra are discussed.

<sup>1</sup>Center for Magnetic Resonance Research and Department of Radiology, University of Minnesota Medical School, Minneapolis, Minnesota, USA.

<sup>2</sup>Department of Chemistry and Chemical Biology, Harvard University, Cambridge, Massachusetts, USA.

<sup>3</sup>Commissariat à l'Énergie Atomique, Service Hospitalier Frédéric Joliot, Orsay, France.

Grant sponsor: NIH; Grant numbers: P41RR00789; R01NS38672; Grant sponsors: MIND Institute; Keck Foundation.

\*Correspondence to: Pierre-Gilles Henry, Center for Magnetic Resonance Research, 2021 6th St. SE, Minneapolis, MN 55455. E-mail: henry@cmrr.umn.edu

Presented in part at the 13th Annual Meeting of ISMRM, Miami, 2005 (abstract #57). An independent study of strong <sup>1</sup>H-<sup>1</sup>H coupling effects in <sup>13</sup>C detection with <sup>1</sup>H localized polarization transfer was presented during the same meeting by A. Yahya and P.S. Allen (abstract #344).

Received 2 June 2005; revised 29 September 2005; accepted 4 October 2005.

DOI 10.1002/mrm.20764

Published online 9 January 2006 in Wiley InterScience (www.interscience.wiley.com).

© 2006 Wiley-Liss, Inc.

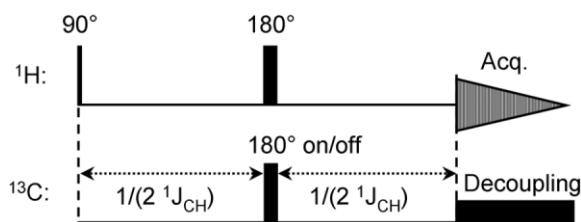


FIG. 1. POCE pulse sequence.

## MATERIALS AND METHODS

### Density Matrix Simulations

Density matrix calculations were performed using programs written in-house in Matlab 6.5 (The MathWorks Inc., Natick, MA, USA). The effects of RF pulses, chemical shift, and  $J$ -coupling were calculated according to the solution to the Liouville equation:

$$\rho(t) = e^{-iHt} \rho_0 e^{iHt}$$

using the appropriate Hamiltonian. For example,  $H = \pi I_{1x}$  for evolution of spin 1 following a  $180^\circ$  pulse applied along the x-axis,  $H = \omega I_{2z}$  for evolution of spin 2 under the effect of chemical shift with off-resonance offset  $\omega$ , and  $H = 2\pi J(I_{1x}I_{2x} + I_{1y}I_{2y} + I_{1z}I_{2z})$  for the evolution of spins 1 and 2 under the effect of (strong)  $J$ -coupling (where the operators for spin  $n$  are  $I_{nx}$ ,  $I_{ny}$ ,  $I_{nz}$ ).

We simulated the free induction decay (FID) signal by calculating the observable signal at each time point during the acquisition time using the equation

$$S(t) = \text{Trace}[F_+ \rho(t)]$$

where  $F_+$  is the detection operator:  $F_+ = I_x + iI_y$ .

Finally, we multiplied the time domain signal by a decaying exponential ( $\exp[-\pi \cdot \text{LB} \cdot t]$ , where LB is the line-broadening in Hz) to obtain Lorentzian lines.  $T_1$  and  $T_2$  relaxation effects during the pulse sequence were neglected.

### Simulation of POCE Spectra

The effect of the POCE pulse sequence (Fig. 1) was evaluated on two different spin systems. The first spin system examined was a simple hypothetical CH-CH system with two protons and two carbons, with one or both of the two carbons being  $^{13}\text{C}$ -labeled. The parameters chosen for this spin system were  $\delta_{\text{H1}} = 2.34$  ppm and  $\delta_{\text{H2}} = 2.09$  ppm, with the representative couplings  $^3J_{\text{HH}} = 7$  Hz and  $^1J_{\text{CH}} = 130$  Hz. POCE spectra were simulated at 63 MHz (1.5 T) using the sequence shown in Fig. 1.

The second, simulated spin system was that of  $[3-^{13}\text{C}]\text{glutamate}$  ( $-\text{CH}-^{13}\text{CH}_2-\text{CH}_2-$ ) with chemical shift and  $^1\text{H}-^1\text{H}$   $J$ -coupling values taken from Govindaraju et al. (16). The one-bond coupling between H3 protons and the C3 carbon of glutamate was taken as  $^1J_{\text{CH}} = 130$  Hz based on measurements of natural abundance  $^{13}\text{C}$  spectra of glutamate. Much smaller long-range (two- and three-bond)  $J_{\text{CH}}$  couplings were neglected. The H4 multiplet corresponding to the natural abundance of  $^{13}\text{C}$  at C4 was accounted

for by simulating the POCE spectra for the doubly labeled isotopomer  $[3,4-^{13}\text{C}_2]\text{glutamate}$ , because nearly all of isotopomers with  $^{13}\text{C}$  at C4 are also labeled at C3. These spectra were scaled to the corresponding isotopomers level of 1.09% before they were added to the simulated  $[3-^{13}\text{C}]\text{glutamate}$  POCE spectra.

All simulations were performed under the assumption that  $^{13}\text{C}$  decoupling was applied during the acquisition time. Perfect decoupling was simulated by removing the heteronuclear  $J$ -coupling term in the Hamiltonian for the acquired signal.

### NMR Spectroscopy

Experimental POCE spectra of 99%-enriched  $[3-^{13}\text{C}]\text{glutamate}$  (Isotec, Miamisburg, OH, USA) were obtained at 200, 400, and 600 MHz on three different Varian high-resolution NMR spectrometers.  $[3-^{13}\text{C}]\text{Glutamate}$  was prepared as a 73 mM solution in 99%  $\text{D}_2\text{O}$  (Cambridge Isotope Laboratories) containing 25 mM phosphate buffer at pH = 6.6, corresponding to pD = 7. The temperature was maintained at  $37^\circ\text{C}$  for 400 and 600 MHz data, and at ambient temperature for 200 MHz data (no temperature control was available). Changes in glutamate chemical shifts between  $20^\circ\text{C}$  and  $37^\circ\text{C}$  were verified to have a negligible effect on the spectral pattern of glutamate at 200 MHz.

The acquisition time was 1 s for 200 and 600 MHz data, and 250 ms for 400 MHz data.

## RESULTS

### CH-CH Model Spin System

Theoretical calculations and simulations of POCE on a simple hypothetical CH-CH spin system clearly demonstrated how strong coupling effects influence the editing selectivity of POCE (Fig. 2).

In the case of a  $^{12}\text{CH}-^{13}\text{CH}$  spin system (in which only one of the two carbons is labeled), the proton spin-echo spectrum without  $^{13}\text{C}$  inversion exhibited the “roof effect” that is characteristic of strongly coupled systems (Fig. 2a, top trace). When the  $^{13}\text{C}$  inversion pulse was applied, only the doublet corresponding to the proton bound to  $^{13}\text{C}$  was inverted (Fig. 2a, middle trace). However, the  $^{13}\text{C}$   $180^\circ$  pulse also “equalized” resonance intensities in each doublet, eliminating the roof effect. Therefore, the resulting difference POCE spectrum exhibited a residual antiphase proton signal at 2.34 ppm even though this proton was attached to  $^{12}\text{C}$  (Fig. 2a, bottom trace). In this case of two CH groups the *integral* over the antiphase doublet was zero so that no error in the calculated  $^{13}\text{C}$  enrichment would occur if the NMR signals were quantified with the use of integration.

These numerical simulations were in excellent agreement with theoretical predictions (see Appendix for detailed calculations). When no  $^{13}\text{C}$  inversion pulse is applied, the density matrix before acquisition is  $(I_{1x} + I_{2x})$ , yielding spectra with unequal resonance intensities characteristic of evolution under strong coupling. When a  $^{13}\text{C}$  inversion is applied, the density matrix before acquisition is  $(I_{1x} - I_{2x})$ , yielding four lines of identical intensities, two of which are inverted.

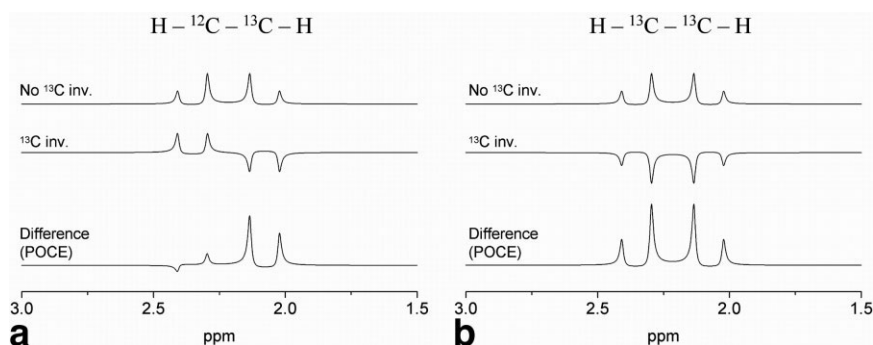


FIG. 2. Simulation of POCE spectra for two hypothetical CH-CH spin systems in which the two protons are strongly coupled (see Materials and Methods for details): (a) only the carbon attached to the proton at 2.09 ppm is a carbon-13 ( $^{12}\text{CH}-^{13}\text{CH}$  spin system), and (b) both carbons are carbon-13 ( $^{13}\text{CH}-^{13}\text{CH}$  spin system). The top trace is obtained for a  $^1\text{H}$  spin echo without  $^{13}\text{C}$  inversion, the middle trace is obtained with  $^{13}\text{C}$  inversion, and the bottom trace is the difference (POCE). Note that in the first case (only one carbon is labeled) significant signal intensities for the proton at 2.34 ppm are detected in the POCE spectrum, even though the corresponding carbon is the  $^{12}\text{C}$  isotope.

The simulations provided virtually identical results regardless of whether  $^1\text{H}$  homonuclear  $J$ -coupling terms were included in the Hamiltonian during the short echo time (TE) of  $1/J_{\text{CH}}$  (results not shown). This justified the neglect of  $J_{\text{HH}}$  during the spin-echo evolution in the theoretical calculations (see Appendix).

In the case of a  $^{13}\text{CH}-^{13}\text{CH}$  spin system (in which both carbons are  $^{13}\text{C}$ -labeled), doublets from both protons were inverted by the  $^{13}\text{C}$  inversion pulse, but this time the strong coupling spectral pattern was unaffected by the  $^{13}\text{C}$  pulse (Fig. 2b, middle trace). The spectral pattern of the POCE difference spectrum (Fig. 2b, bottom trace) was therefore identical to the spectral pattern of the reference spin-echo spectrum. Again, this was in agreement with theoretical calculations. When both carbons are labeled, the density matrix before acquisition is  $-(I_{1x} + I_{2x})$ , and the resulting spectrum is identical to the spin-echo spectrum but inverted.

In the general case, in which each of the two carbon positions may be  $^{13}\text{C}$ -labeled and the isotopic enrichment of each carbon can be denoted as  $p$  and  $q$ , respectively (with random distribution of  $^{13}\text{C}$  label on each carbon), the relative proportions of  $^{12}\text{CH}-^{12}\text{CH}$ ,  $^{13}\text{CH}-^{12}\text{CH}$ ,  $^{12}\text{CH}-^{13}\text{CH}$ , and  $^{13}\text{CH}-^{13}\text{CH}$  molecules are  $(1-p)(1-q)$ ,  $p(1-q)$ , and  $(1-p)q$  and  $pq$ , respectively. The resulting POCE spectrum derives from the following density matrix before acquisition:

$$(I_{1x} + I_{2x}) - (1-p)(1-q)(I_{1x} + I_{2x}) - (1-p)q(I_{1x} - I_{2x}) \\ - p(1-q)(-I_{1x} + I_{2x}) + pq(I_{1x} + I_{2x})$$

or

$$(I_{1x} + I_{2x})[p + q] + (I_{1x} - I_{2x})[p - q]$$

Therefore, when each carbon has the same fractional enrichment ( $p = q$ ), the POCE spectrum has the same spectral pattern as the spin-echo spectrum without  $^{13}\text{C}$  inversion. This situation also applies to the natural-abundance case in which  $p = q = 1.1\%$ . In contrast, when the two carbon sites have different enrichments ( $p \neq q$ ), the term  $(I_{1x} - I_{2x})$  introduces a partial equalization of resonance intensi-

ties in each doublet in the POCE spectrum compared to the unedited spectrum.

### Glutamate Spin System

Simulated POCE spectra for the isotopomers corresponding to 99%  $[3-^{13}\text{C}]$ glutamate confirmed the presence of a significant signal from H4 protons that were not bound to  $^{13}\text{C}$  at 2.34 ppm (Fig. 3c), which was much larger than the natural abundance level (Fig. 3d). This signal was more prominent at lower field strength, consistent with the fact that strong coupling effects are more pronounced at lower field. More specifically, the ratio of the residual POCE signal (integrated from 2.25 ppm to 2.45 ppm on the real part of the spectrum) relative to the H4 signal for the case of  $^{13}\text{C}$  at natural abundance was about 8 at 200 MHz (4.7 T), 5 at 400 MHz (9.4 T), and 3 at 600 MHz (14.1 T). At 200 MHz the outer components of the Glu-H4 triplet had more nearly equal intensities with than without the  $^{13}\text{C}$  inversion pulse, reminiscent of the strong coupling effects observed on POCE spectra of the  $^{12}\text{CH}-^{13}\text{CH}$  spin system. Note, however, that in the case of a more complex spin system, such as  $[3-^{13}\text{C}]$ glutamate, the residual signal of H4 at 2.34 ppm had some antiphase character, but its integral was not equal to zero, as was the case for a  $^{12}\text{CH}-^{13}\text{CH}$  system. When the strong coupling components were removed from the Hamiltonian, i.e.,  $H = 2\pi J(I_{1z}I_{2z})$  was used instead of  $H = 2\pi J(I_{1x}I_{2x} + I_{1y}I_{2y} + I_{1z}I_{2z})$ , the POCE spectrum showed no signal for H4 (results not shown), confirming that the signal at 2.34 ppm (Fig. 3c) arose from strong coupling effects. In addition, the multiplet for H2 at 3.75 ppm exhibited intensities corresponding to the natural-abundance level of  $^{13}\text{C}$  at C2 (results not shown), consistent with the fact that H2 and H3 protons represent a weakly coupled system at field strengths above  $\sim 2$  T. When both the C3 and C4 carbons of glutamate were labeled, simulations showed that the relative intensities in the POCE spectrum were identical to those of the unedited spectrum (results not shown), as was the case for the  $^{13}\text{CH}-^{13}\text{CH}$  spin system shown in Fig. 2b. Finally, experimental spectra of  $[3-^{13}\text{C}]$ glutamate acquired at 200, 400, and 600 MHz were very similar to simulated spectra (Fig. 3e), confirming the validity of the simulations.

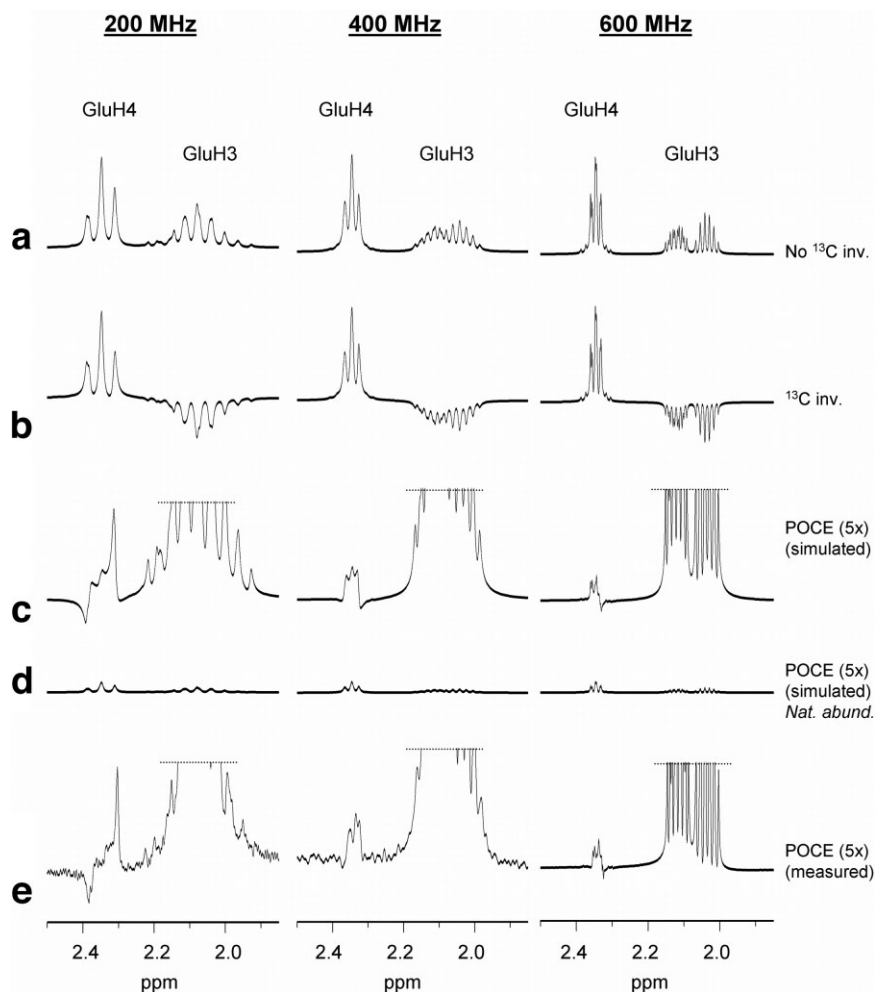


FIG. 3. Simulated and experimental POCE spectra of [3- $^{13}\text{C}$ ]glutamate (98.9% label at C3, 1.1% at C4) at different field strengths (columns). Simulated spin-echo spectra without (a) and with (b)  $^{13}\text{C}$  inversion, and the resulting POCE difference (c = a - b, scaled up five times). d: Simulated POCE spectra of glutamate with 1.1% natural abundance  $^{13}\text{C}$  label at each carbon, presented at the same vertical scale as c. e: Experimental spectra of 99%-enriched [3- $^{13}\text{C}$ ]glutamate. Although glutamate was not enriched at C4 (above natural abundance), significant H4 multiplet intensity was obtained at 2.34 ppm, especially at lower field strength.

## DISCUSSION

The present study demonstrates that the editing selectivity of POCE is affected when POCE is applied to strongly coupled (i.e., second-order) spin systems. In such cases, proton signals can be detected for  $^{12}\text{C}$ - $^1\text{H}$  moieties that are strongly coupled to  $^{13}\text{C}$ - $^1\text{H}$  moieties. The behavior of strongly coupled systems (such as the “virtual coupling” phenomenon (17)) has been reported for 2D NMR spectroscopy (18–21), but to the best of our knowledge has not been studied with 1D heteronuclear editing sequences.

It is important to note that even in the case of strongly coupled systems, the detected signal in POCE spectra still originates only from protons in molecules that contain  $^{13}\text{C}$  carbons. Indeed, signals from molecules that contain no  $^{13}\text{C}$  nuclei are unaffected by the  $^{13}\text{C}$  inversion pulse and are eliminated in the difference spectrum. However, since  $J$ -evolution under strong coupling conditions during the acquisition time causes coherence transfer between protons (mixed eigenstates), a signal is eventually detected for the  $^{12}\text{C}$ - $^1\text{H}$  moiety through coherence transfer from the  $^{13}\text{C}$ - $^1\text{H}$  moiety. We show that this is the case when the two carbons attached to the two protons that are strongly coupled have a different isotopic enrichment. In the particular case in which the isotopic enrichment of both carbons is identical, this effect is exactly canceled, and thus the

POCE spectrum still accurately reflects the isotopic enrichment.

As expected, strong coupling effects in POCE spectra of [3- $^{13}\text{C}$ ]glutamate were more prominent at lower field (200 MHz) than at higher field (600 MHz). Even at 400 MHz (a field strength currently used for  $^{13}\text{C}$  NMR studies in animals), the integral of the glutamate H4 multiplet at 2.34 ppm for [3- $^{13}\text{C}$ ]glutamate (integrated on the real part of the phased spectrum) was five times higher than the natural abundance level. Therefore, in the case of a strongly coupled system with unequal enrichment at the associated carbon sites,  $^1\text{H}$  signal integrals in the POCE spectrum may not directly reflect carbon isotopic enrichment, and strong coupling effects must be taken into account in the quantification.

The increasing use of sophisticated spectral analysis methods, such as LCModel (22), is enabling investigators to perform more precise and user-independent data analyses. The LC modeling approach requires that accurate prior knowledge be provided in the form of “model” spectra that can be either measured or simulated. For example, one way to build a basis set to fit POCE spectra of glutamate is to measure a glutamate spin-echo spectrum (i.e., POCE without  $^{13}\text{C}$  inversion pulse) and split this spectrum into three different parts to obtain model

spectra for glutamate H4, H3, and H2 resonances (8,11). However, in strongly coupled systems this approach may not reproduce all spectral characteristics of POCE spectra, because strong coupling causes spectral patterns in POCE spectra to differ from spectral patterns in unedited spin-echo spectra. Another possible approach is to measure every isotopomer (e.g., [3-<sup>13</sup>C]glutamate, [4-<sup>13</sup>C]glutamate, etc.), but this would be impractical and very costly.

Density matrix simulations therefore appear to be the most attractive and practical approach for obtaining the desired LCModel basis set (23,24). Although in this study in-house-written Matlab programs were used, as in other studies (24), other programs such as GAMMA (25) and NMR-SIM@ (Bruker BioSpin GmbH, Rheinstetten, Germany) are also available. The incorporation of simulated spectra for [3-<sup>13</sup>C]glutamate and [4-<sup>13</sup>C]glutamate into the basis set for LCModel would directly take strong coupling effects into account in the spectral quantification. The use of simulated spectra was previously proposed to quantify <sup>1</sup>H{<sup>13</sup>C} spectra acquired without <sup>13</sup>C decoupling (26). Although the possibility of coherence transfer from one proton to another under strong coupling is not discussed in this paper, individual simulated spectra of [3-<sup>13</sup>C]glutamate and [4-<sup>13</sup>C]glutamate clearly show a multiplet at the proton chemical shift corresponding to the unlabeled carbon, consistent with our findings.

After the initial POCE sequence was introduced, several different sequences were proposed for <sup>1</sup>H-<sup>13</sup>C difference editing that incorporate a <sup>13</sup>C inversion pulse into localization sequences such as stimulated-echo acquisition mode (STEAM) (11), point-resolved spectroscopy (PRESS) (12), or *J*-refocused coherence transfer (13). Semiselective POCE (14) and 2D <sup>1</sup>H{<sup>13</sup>C} detection (27) were also proposed to distinguish the Glu-H3 and Glu-H4 protons bound to <sup>13</sup>C. Strong coupling effects may affect the editing selectivity in these pulse sequences as well, as suggested in a recent abstract (28). However, in a study by Henry et al. (14), glutamate H4 and H3 signals were measured as peak amplitudes, so that any residual signal at a different chemical shift would most likely have a negligible impact on the measured time courses of <sup>13</sup>C label incorporation into glutamate C4 and C3.

Our study focused primarily on the performance of the POCE sequence with <sup>13</sup>C decoupling applied during acquisition. Several other cases (such as analysis of strong coupling effects in POCE without <sup>13</sup>C decoupling, and strong coupling effects in other <sup>13</sup>C-editing sequences with TEs longer than  $1/J_{CH}$ ) were not considered in detail in this study but may be addressed in future work. The effect of long-range couplings and the consequences of a spread in  $J_{CH}$  values could also be considered. Although evolution under carbon-carbon *J*-coupling ( $J_{CC}$ ) for multiply-labeled molecules had no influence on simulated signals in POCE spectra (results not shown) because <sup>13</sup>C spins remain longitudinal throughout the pulse sequence,  $J_{CC}$  would have to be taken into account in pulse sequences in which <sup>13</sup>C spins are flipped into the transverse plane.

Coherence transfer between strongly coupled protons should increase with increasing echo delay, and our simulations indicate that strong coupling effects are more pronounced when TEs longer than  $1/J_{CH}$  are used (results not shown), such as in <sup>13</sup>C-PRESS (12) or <sup>13</sup>C-Localization by Adiabatic Selective Refocusing (LASER) (29,30). In these sequences, in which the <sup>13</sup>C inversion is placed either  $1/(2 J_{CH})$  after excitation or  $1/(2 J_{CH})$  before acquisition, the TE is generally significantly longer than that in the POCE sequence, and thus evolution under homonuclear *J*-coupling during the TE can no longer be neglected. Simulations indicate that strong coupling effects become particularly pronounced if the <sup>13</sup>C pulse is placed  $1/(2 J_{CH})$  after the excitation pulse, as opposed to  $1/(2 J_{CH})$  before the acquisition (results not shown).

Accurate quantification of POCE spectra is critical for in vivo metabolic studies in which time courses of <sup>13</sup>C label incorporation are measured and analyzed to obtain quantitative metabolic fluxes (e.g., to elucidate brain energy metabolism and glutamatergic neurotransmission). In such studies inaccurate quantification of isotopic enrichment could potentially lead to a systematic bias in the analysis. The ultimate impact of strong coupling effects on the detection of <sup>13</sup>C labeling time courses remains to be determined. It will depend not only on the  $B_0$  field strength used to detect the NMR signals, but also on the particular pulse sequence and spectral quantification method employed to detect and analyze the POCE spectra.

## CONCLUSIONS

We conclude that for strongly coupled spin systems, proton signal integrals in POCE spectra do not accurately reflect the true <sup>13</sup>C enrichment of the attached carbons when the levels of enrichment are not equal at all carbon positions. This situation applies, for example, to glutamate, in which case the protons bound to carbons C3 and C4 are strongly coupled at the magnetic fields typically used for in vivo studies. These difficulties may be overcome by incorporating adequate prior knowledge (e.g., simulated spectra of the isotopomers) into the spectral analysis.

## ACKNOWLEDGMENTS

We thank Prof. Michael Garwood and Dr. Vincent Lebon for useful discussions during the preparation of this manuscript. The high-resolution NMR facility at the University of Minnesota is supported by funds from the NSF (BIR-961477), the University of Minnesota Medical School, and the Minnesota Medical Foundation. We also acknowledge the 3M Corporation and the Department of Chemistry, University of Minnesota, for the use of their 400 and 200 MHz spectrometers, respectively.

## APPENDIX

Theoretical Calculation of POCE Spectra for a Strongly Coupled  $^{12}\text{C}\text{H}-^{13}\text{C}\text{H}$  Spin System

## Definition of Strong Coupling

The definition of a strongly coupled system requires clarification in the case of a heteronuclear spin system.

A strongly coupled spin system occurs when the smallest difference in the resonance frequencies (multiplet components) of two mutually coupled protons approaches the magnitude of their  $J$ -coupling. The separation between multiplets is determined by their chemical shift difference  $\Delta\delta$  in combination with any heteronuclear  $J$  couplings that may be involved. In the strong coupling case  $J_{\text{HH}}$  evolution cannot in general be approximated by using the Hamiltonian  $H_z = 2\pi J_{1z}I_{2z}$  and the full  $J$ -coupling Hamiltonian  $H = 2\pi \mathbf{I}_1 \cdot \mathbf{I}_2 = 2\pi(J_{1x}I_{2x} + I_{1y}I_{2y} + I_{1z}I_{2z})$  must be used.

## Density Matrices Before Acquisition

Let  $\mathbf{I}_1$  and  $\mathbf{I}_2$  be operators for proton spins 1 and 2, respectively, where spin 2 is attached to a  $^{13}\text{C}$  atom.

In the following calculation, the evolution due to the homonuclear scalar coupling  $J_{\text{HH}} \ll J_{\text{CH}}$  is ignored during the TE.

When no  $^{13}\text{C}$   $180^\circ$  pulse is applied, the density matrix just before acquisition is given by

$$\rho_1(\tau) = I_{1x} + I_{2x}$$

since in this case the evolution under chemical shifts and heteronuclear coupling is assumed to be completely refocused by the  $180^\circ$  pulse on the protons.

When the  $^{13}\text{C}$   $180^\circ$  pulse is applied exactly at time  $\tau = 1/(2 J_{\text{CH}})$ , the density matrix at the beginning of data acquisition ( $^1\text{H}$  signal) is given by

$$\rho_2(\tau) = I_{1x} - I_{2x}$$

Spectra Resulting From  $^1\text{H}$  Data Acquisition

The Hamiltonian in the rotating frame during acquisition (assuming that  $^{13}\text{C}$  decoupling removes heteronuclear scalar coupling) is given by

$$H = 2\pi \mathbf{I}_1 \cdot \mathbf{I}_2 + \omega_1 I_{1z} + \omega_2 I_{2z}$$

where  $\omega_1$  and  $\omega_2$  are the proton chemical shifts, and  $J$  is the homonuclear scalar coupling between spins 1 and 2.

In matrix form,  $H$  can be written in the basis  $|\alpha, \alpha\rangle, |\alpha, \beta\rangle, |\beta, \alpha\rangle, |\beta, \beta\rangle$  as

$$H = \begin{pmatrix} J' + \Sigma_{12} & 0 & 0 & 0 \\ 0 & \Delta_{12} - J' & 2J' & 0 \\ 0 & 2J' & -\Delta_{12} - J' & 0 \\ 0 & 0 & 0 & J' - \Sigma_{12} \end{pmatrix}$$

where

$$J' = \frac{\pi J}{2}$$

$$\Sigma_{12} = \frac{(\omega_1 + \omega_2)}{2}$$

$$\Delta_{12} = \frac{(\omega_1 - \omega_2)}{2}$$

The corresponding eigenvalues and eigenvectors are given by

$$|\Psi_1\rangle = |\alpha, \alpha\rangle$$

$$|\Psi_2\rangle = \cos\theta |\alpha, \beta\rangle + \sin\theta |\beta, \alpha\rangle$$

$$|\Psi_3\rangle = -\sin\theta |\alpha, \beta\rangle + \cos\theta |\beta, \alpha\rangle$$

$$|\Psi_4\rangle = |\beta, \beta\rangle$$

$$E_1 = J' + \Sigma_{12}$$

$$E_2 = -J' + \sqrt{4J'^2 + \Delta_{12}^2}$$

$$E_3 = -J' - \sqrt{4J'^2 + \Delta_{12}^2}$$

$$E_4 = J' - \Sigma_{12}$$

where

$$\cos\theta = \frac{2J'}{\sqrt{4J'^2 + (\sqrt{4J'^2 + \Delta_{12}^2} - \Delta_{12})^2}}$$

$$\sin\theta = \frac{\sqrt{4J'^2 + \Delta_{12}^2} - \Delta_{12}}{\sqrt{4J'^2 + (\sqrt{4J'^2 + \Delta_{12}^2} - \Delta_{12})^2}}$$

Note that when  $\Delta_{12} \gg J'$ ,  $\cos\theta \rightarrow 1$ , and the results for weak coupling are obtained.

The propagator for time  $t$  is given by

$$U(t) = \exp(-iHt) = V\tilde{U}(t)V^\dagger = V \begin{pmatrix} \exp(-iE_1t) & 0 & 0 & 0 \\ 0 & \exp(-iE_2t) & 0 & 0 \\ 0 & 0 & \exp(-iE_3t) & 0 \\ 0 & 0 & 0 & \exp(-iE_4t) \end{pmatrix} V^\dagger$$

$$\text{where } V = \begin{pmatrix} 1 & 0 & 0 & 0 \\ 0 & \cos\theta & -\sin\theta & 0 \\ 0 & \sin\theta & \cos\theta & 0 \\ 0 & 0 & 0 & 1 \end{pmatrix}$$

For the initial condition

$$\rho_1(0) = I_{1x} + I_{2x}$$

the corresponding FID,  $S(t)$ , is given by

---


$$\begin{aligned} S(t) &= \text{Tr}[I_+ U(t)\rho(0)U^\dagger(t)] \\ &= \text{Tr}[V^\dagger I_+ V \tilde{U}(t) V^\dagger \rho(0) V \tilde{U}^\dagger(t)] \\ &= \text{Tr} \left[ \begin{pmatrix} 0 & c_s & c_d & 0 \\ 0 & 0 & 0 & c_s \\ 0 & 0 & 0 & c_d \\ 0 & 0 & 0 & 0 \end{pmatrix} \begin{pmatrix} 0 & c_s \exp(i\omega_{21}t) & c_d \exp(i\omega_{31}t) & 0 \\ c_s \exp(i\omega_{12}t) & 0 & 0 & c_s \exp(i\omega_{42}t) \\ c_d \exp(i\omega_{13}t) & 0 & 0 & c_d \exp(i\omega_{43}t) \\ 0 & c_s \exp(i\omega_{24}t) & c_d \exp(i\omega_{34}t) & 0 \end{pmatrix} \right] \\ &= c_s^2 (\exp(i\omega_{12}t) + \exp(i\omega_{24}t)) + c_d^2 (\exp(i\omega_{13}t) + \exp(i\omega_{34}t)) \end{aligned}$$


---

where  $c_d = \cos\theta - \sin\theta$ ,  $c_s = \cos\theta + \sin\theta$ , and  $\omega_{ij} = E_i - E_j$ .

The resulting spectra consist of four peaks at frequencies  $\omega_{12}$ ,  $\omega_{24}$ ,  $\omega_{13}$ , and  $\omega_{34}$ , with intensities  $c_s^2$ ,  $c_s^2$ ,  $c_d^2$ , and  $c_d^2$ . This spectrum shows the so-called ‘‘roof effect’’ that is characteristic of strongly coupled systems.

For the initial condition,

$$\rho_2(0) = I_{1x} - I_{2x}$$

The resulting FID is given by

---


$$\begin{aligned} S(t) &= \text{Tr}[I_+ U(t)\rho(0)U^\dagger(t)] \\ &= \text{Tr}[V^\dagger I_+ V \tilde{U}(t) V^\dagger \rho(0) V \tilde{U}^\dagger(t)] \\ &= \text{Tr} \left[ \begin{pmatrix} 0 & c_s & c_d & 0 \\ 0 & 0 & 0 & c_s \\ 0 & 0 & 0 & c_d \\ 0 & 0 & 0 & 0 \end{pmatrix} \begin{pmatrix} 0 & -c_d \exp(i\omega_{21}t) & c_s \exp(i\omega_{31}t) & 0 \\ -c_d \exp(i\omega_{12}t) & 0 & 0 & c_d \exp(i\omega_{42}t) \\ c_s \exp(i\omega_{13}t) & 0 & 0 & -c_s \exp(i\omega_{43}t) \\ 0 & c_d \exp(i\omega_{24}t) & -c_s \exp(i\omega_{34}t) & 0 \end{pmatrix} \right] \\ &= c_s c_d (\exp(i\omega_{13}t) + \exp(i\omega_{24}t) - \exp(i\omega_{12}t) - \exp(i\omega_{34}t)) \end{aligned}$$


---

The peak intensities are all equal ( $c_s c_d$ ), and the two transitions that are nominally associated with spin 2 ( $\omega_{12}$ ,  $\omega_{34}$ ) are inverted relative to the transitions of spin 1 ( $\omega_{13}$ ,  $\omega_{24}$ ).

## REFERENCES

- Gruetter R, Adriany G, Choi I-Y, Henry P-G, Lei H-X, Oz G. Localized in vivo  $^{13}\text{C}$  NMR spectroscopy of the brain. *NMR Biomed* 2003;16:313–338.
- Novotny EJ, Ogino T, Rothman DL, Petroff OAC, Prichard JW, Shulman RG. Direct carbon versus proton heteronuclear editing of 2- $^{13}\text{C}$  ethanol in rabbit brain in vivo: a sensitivity comparison. *Magn Reson Med* 1990;16:431–443.
- Gruetter R, Seaquist ER, Ugurbil K. A mathematical model of compartmentalized neurotransmitter metabolism in the human brain. *Am J Physiol* 2001;281:E100–E112.
- Henry P-G, Tkac I, Gruetter R.  $^1\text{H}$ -localized broadband  $^{13}\text{C}$  NMR spectroscopy of the rat brain in vivo at 9.4 Tesla. *Magn Reson Med* 2003;50:684–692.
- Henry P-G, Oz G, Provencher S, Gruetter R. Toward dynamic isotopomer analysis in the rat brain in vivo: automatic quantitation of  $^{13}\text{C}$  NMR spectra using LCMoDel. *NMR Biomed* 2003;16:400–412.
- Hyder F, Rothman DL, Mason GF, Rangarajan A, Behar KL, Shulman RG. Oxidative glucose metabolism in rat brain during single forepaw stimulation: a spatially localized  $^1\text{H}$ [ $^{13}\text{C}$ ] nuclear magnetic resonance study. *J Cereb Blood Flow Metab* 1997;17:1040–1047.

7. Chen W, Zhu XH, Gruetter R, Seaquist ER, Adriany G, Ugurbil K. Study of tricarboxylic acid cycle flux changes in human visual cortex during hemifield visual stimulation using  $^1\text{H}$ - $^{13}\text{C}$  MRS and fMRI. *Magn Reson Med* 2001;45:349–355.
8. de Graaf RA, Mason GF, Patel AB, Rothman DL, Behar KL. Regional glucose metabolism and glutamatergic neurotransmission in rat brain in vivo. *Proc Natl Acad Sci USA* 2004;101:12700–12705.
9. Mason GF, Pan JW, Chu W-J, Newcomer BR, Zhang Y, Orr R, Hetherington HP. Measurement of the tricarboxylic acid cycle rate in human grey and white matter in vivo by  $^1\text{H}$ - $^{13}\text{C}$  magnetic resonance spectroscopy at 4.1T. *J Cereb Blood Flow Metab* 1999;19:1179–1188.
10. Rothman DL, Behar KL, Hetherington HP, den Hollander JA, Bendall MR, Petroff OAC, Shulman RG.  $^1\text{H}$ -observe/ $^{13}\text{C}$ -decouple spectroscopic measurements of lactate and glutamate in the rat brain in vivo. *Proc Natl Acad Sci USA* 1985;82:1633–1637.
11. Pfeuffer J, Tkac I, Choi I-Y, Merkle H, Ugurbil K, Garwood M, Gruetter R. Localized in vivo  $^1\text{H}$  NMR detection of neurotransmitter labeling in rat brain during infusion of  $[1-^{13}\text{C}]$  D-glucose. *Magn Reson Med* 1999;41:1077–1083.
12. Chen W, Adriany G, Zhu X-H, Gruetter R, Ugurbil K. Detecting natural abundance carbon signal of NAA metabolite within  $12\text{-cm}^3$  localized volume of human brain  $^1\text{H}$ - $^{13}\text{C}$  NMR spectroscopy. *Magn Reson Med* 1998;40:180–184.
13. Pan JW, Mason GF, Vaughan JT, Chu WJ, Zhang Y, Hetherington HP.  $^{13}\text{C}$  editing of glutamate in human brain using J-refocused coherence transfer spectroscopy at 4.1 T. *Magn Reson Med* 1997;37:355–358.
14. Henry P-G, Roussel R, Vaufrey F, Dautry C, Bloch G. Semiselective POCE NMR spectroscopy. *Magn Reson Med* 2000;44:395–400.
15. Freeman R, Mareci TH, Morris GA. Weak satellite signals in high-resolution NMR spectra: separating the wheat from the chaff. *J Magn Reson* 1981;42:341–345.
16. Govindaraju V, Young K, Maudsley AA. Proton NMR chemical shifts and coupling constants for brain metabolites. *NMR Biomed* 2000;13:129–153.
17. Morris GA, Smith KI. “Virtual coupling” in heteronuclear chemical-shift correlation by two-dimensional NMR. A simple test. *J Magn Reson* 1985;65:506–509.
18. Freeman R, Morris GA, Turner DL. Proton-coupled carbon-13 *J* spectra in the presence of strong coupling. I. *J Magn Reson* 1977;26:373–378.
19. Bodenhausen G, Freeman R, Morris GA, Turner DL. Proton-coupled carbon-13 *J* spectra in the presence of strong coupling. II. *J Magn Reson* 1977;28:17–28.
20. Kumar A. Two-dimensional spin-echo NMR spectroscopy: a general method for calculation of spectra. *J Magn Reson* 1978;30:227–249.
21. Hull WE. Experimental aspects of two-dimensional NMR. In: Crossman WR, Carlson MK, editors. *Two-dimensional NMR spectroscopy*. 2nd ed. New York: John Wiley & Sons; 1994. p 263, 383, 407.
22. Provencher S. Estimation of metabolite concentrations from localized in vivo proton NMR spectra. *Magn Reson Med* 1993;30:672–679.
23. Young K, Govindaraju V, Soher BJ, Maudsley AA. Automated spectral analysis. I. Formation of a priori information by spectral simulation. *Magn Reson Med* 1998;40:812–815.
24. Thompson RB, Allen PS. Response of metabolites with coupled spins to the STEAM sequence. *Magn Reson Med* 2001;45:955–965.
25. Smith SA, Levante TO, Meier BH, Ernst RR. Computer simulations in magnetic resonance. An object-oriented programming approach. *J Magn Reson Ser A* 1994;106:75–105.
26. Boumezbeur F, Besret L, Valette J, Vaufrey F, Henry PG, Slavov V, Giacomini E, Hantraye P, Bloch G, Lebon V. NMR measurement of brain oxidative metabolism in monkeys using  $^{13}\text{C}$ -labeled glucose without a  $^{13}\text{C}$  radiofrequency channel. *Magn Reson Med* 2004;52:33–40.
27. Watanabe H, Ishihara Y, Okamoto K, Oshio K, Kanamatsu T, Tsukada Y. 3D localized  $^1\text{H}$ - $^{13}\text{C}$  heteronuclear single-quantum coherence correlation spectroscopy in vivo. *Magn Reson Med* 2000;43:200–210.
28. Yahya A, Allen PS. 3D localized direct  $^{13}\text{C}$  detection using PRESS and a modified DEPT sequence. In: *Proceedings of the 13th Annual Meeting of ISMRM, Miami Beach, FL, USA, 2005*. p 344.
29. Garwood M, DelaBarre L. The return of the frequency sweep: designing adiabatic pulses for contemporary NMR. *J Magn Reson* 2001;153:155–177.
30. Marjanska M, Henry P-G, Gruetter R, Garwood M, Ugurbil K. A new method for proton detected carbon edited spectroscopy using LASER. In: *Proceedings of the 12th Annual Meeting of ISMRM, Kyoto, Japan, 2004*. p 679.